University Medical Center Rotterdam (NL45264.078.13).

AUTHOR CONTRIBUTIONS

Conceptualization: EP; Data Curation: EF; Formal Analysis: AV, KvS; Methodology: EF, EP; Investigation: EF; Visualization; KvS; Writing - Original Draft Preparation: AV, KvS; Writing - Review and Editing: AV, EP, KvS.

Allard R.J.V. Vossen[1,*], Kelsey R. van Straalen[1], Edwin F. Florencia[1] and Errol P. Prens[1]

[1]*Department of Dermatology, Erasmus University Medical Center, Rotterdam, the Netherlands*
[*]*Corresponding author e-mail: a.vossen@erasmusmc.nl*

SUPPLEMENTARY MATERIAL

Supplementary material is linked to the online version of the paper at www.jidonline.org, and at https://doi.org/10.1016/j.jid.2020.01.023.

REFERENCES

Cayrol C, Girard JP. Interleukin-33 (IL-33): a nuclear cytokine from the IL-1 family. Immunol Rev 2018;281:154–68.

Contassot E, Beer HD, French LE. Interleukin-1, inflammasomes, autoinflammation and the skin. Swiss Med Wkly 2012;142:w13590.

Frew JW. Commentary: hidradenitis suppurativa: A systematic review integrating inflammatory pathways into a cohesive pathogenic model. Front Immunol 2019;10:302.

Jenei A, Dajnoki Z, Medgyesi B, Gáspár K, Béke G, Á Kinyó, et al. Apocrine gland-rich skin has a non-inflammatory IL-17-related immune milieu, that turns to inflammatory IL-17-mediated disease in hidradenitis suppurativa. J Invest Dermatol 2019;139:964–8.

Kelly G, Hughes R, McGarry T, van den Born M, Adamzik K, Fitzgerald R, et al. Dysregulated cytokine expression in lesional and nonlesional skin in hidradenitis suppurativa. Br J Dermatol 2015;173:1431–9.

Takatsu K, Kouro T, Nagai Y. Interleukin 5 in the link between the innate and acquired immune response. Adv Immunol 2009;101:191–236.

Van der Zee HH, De Ruiter L, Boer J, Van Den Broecke DG, Den Hollander JC, Laman JD, et al. Alterations in leucocyte subsets and histomorphology in normal-appearing perilesional skin and early and chronic hidradenitis suppurativa lesions. Br J Dermatol 2012;166:98–106.

Vossen A, Ardon CB, van der Zee HH, Lubberts E, Prens EP. The anti-inflammatory potency of biologics targeting TNF-α, interleukin (IL)-17A, IL-12/23 and CD 20 in hidradenitis suppurativa: an ex vivo study. Br J Dermatol 2019;181:312–23.

Vossen ARJV, Schoenmakers A, van Straalen KR, Prens EP, van der Zee HH. Assessing pruritus in hidradenitis suppurativa: a cross-sectional study. Am J Clin Dermatol 2017;18:687–95.

Vossen ARJV, van der Zee HH, Prens EP. Hidradenitis suppurativa: a systematic review integrating inflammatory pathways into a cohesive pathogenic model. Front Immunol 2018;9:2965.

Witte-Händel E, Wolk K, Tsaousi A, Irmer ML, Mößner R, Shomroni O, et al. The IL-1 pathway is hyperactive in hidradenitis suppurativa and contributes to skin infiltration and destruction. J Invest Dermatol 2019;139:1294–305.

Cutaneous T-Cell Lymphoma (CTCL) Cell Line-Derived Extracellular Vesicles Contain HERV-W-Encoded Fusogenic Syncytin-1

Journal of Investigative Dermatology (2020) **140,** 1466–1469; doi:10.1016/j.jid.2019.11.021

TO THE EDITOR

We have previously shown that human endogenous retrovirus-W-encoded fusogenic membrane protein syncytin-1 plays a role in the pathogenesis of mycosis fungoides (MF), the most common primary cutaneous T-cell lymphoma (CTCL) (Maliniemi et al., 2013). The expression of syncytin-1 protein was detected in 15 of 30 MF skin lesions but not in skin-homing nonmalignant lymphocytes. Primary cutaneous CD30-positive lymphoproliferative disorders, including lymphomatoid papulosis and primary cutaneous anaplastic large cell lymphoma, are the second most common form of CTCLs and represent approximately 25% of all CTCLs (Nikolaenko et al., 2019; Willemze et al., 2019). This study examined the expression and functional properties of syncytin-1 in verified cell lines of the aforementioned forms of CTCLs and also its presence in the extracellular vesicles (EVs) released by the malignant cells.

Human endogenous retrovirus-driven syncytin-1 expression is upregulated in a wide variety of human malignancies, such as rectal and colorectal cancer, prostate cancer, bladder cancer, leukemia, and lymphoma (Bastida-Ruiz et al., 2016). Functionally, upregulated syncytin-1 has been shown to promote the cell-to-cell fusion of endometrial carcinoma cells (Strick et al., 2007) and breast cancer or squamous cell carcinoma cells to endothelial cells (Bjerregaard et al., 2006). Despite these observations, the role of syncytin-1 in cancer remains poorly understood.

EVs contain a variety of proteins, lipids, RNAs, and DNA and have recently emerged as an important form of intercellular communication in cancer (Yáñez-Mó et al., 2015). Malignant cell-derived EVs can be released into the circulation and transfer their contents to nontumor cells to reprogram target cell function or to prepare metastatic niches (Maas et al., 2017). The current knowledge on the molecular mechanisms of the fusogenic properties of EVs are not yet fully characterized, but syncytins are anticipated to be involved in the binding of EVs to target cells, a process preceding fusion (Prada and Meldolesi, 2016).

Using immunocytochemistry and western blot analyses (Supplementary Materials), we observed that both the syncytin-1 protein (Figure 1) and its receptors ASCT1 and ASCT2 (Supplementary Figure S1) are expressed in CTCL cell lines representing MF (MyLa cell line), lymphomatoid

Abbreviations: CTCL, cutaneous T-cell lymphoma; EV, extracellular vesicle; MF, mycosis fungoides

Accepted manuscript published online 26 December 2019; corrected proof published online 17 January 2020

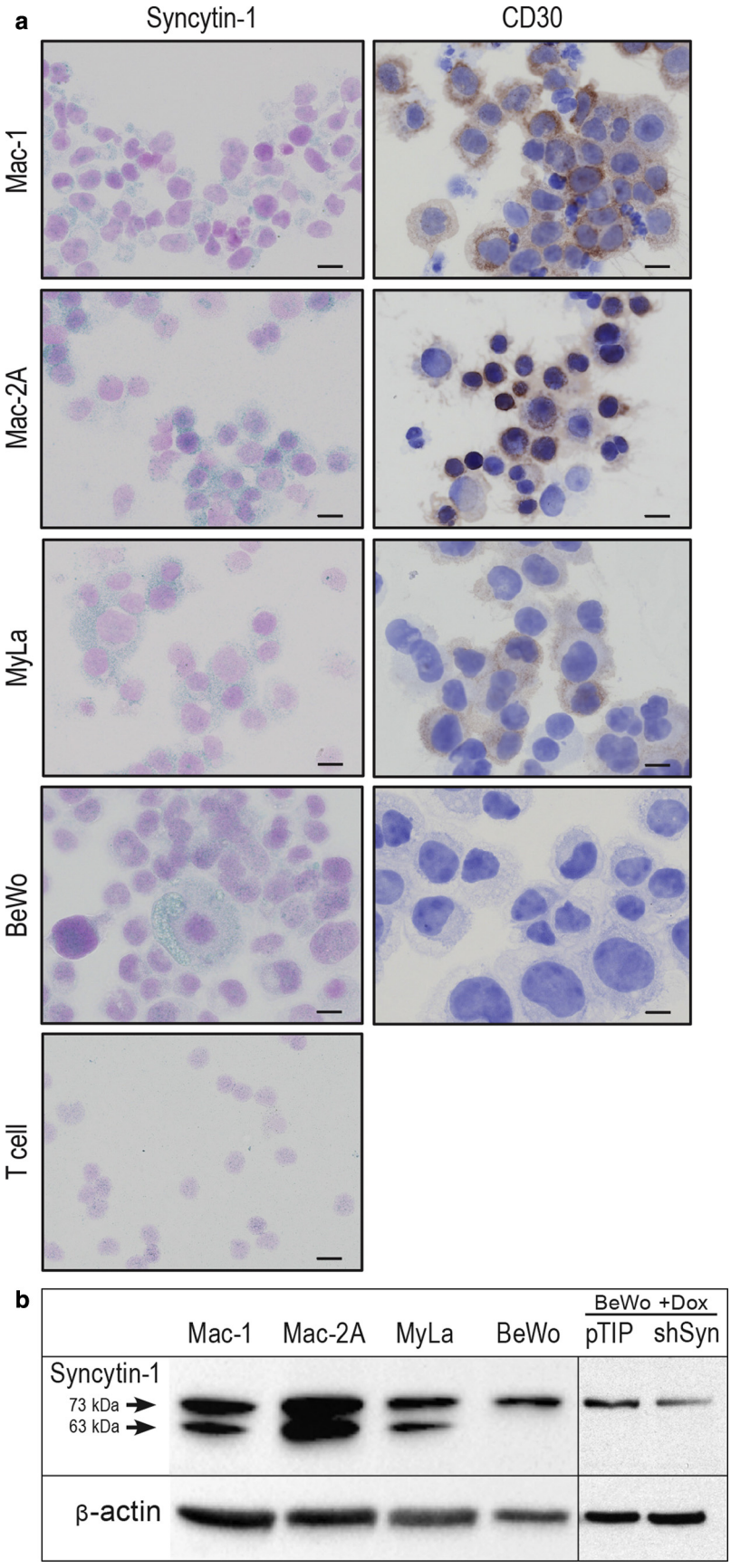

Figure 1. Syncytin-1 and CD30 are expressed in CTCL cell lines. (**a**) The left-hand panel shows high expression of syncytin-1 (turquoise) in the CTCL and BeWo cell lines as detected by immunocytochemistry. Normal T cells as reference. The right-hand panel shows CD30 (dark brown) expression in the Mac-1, Mac-2A, and MyLa cell lines but not in BeWo cells. Bar = 20 μm. (**b**) Western blot analysis of CTCL and BeWo cell lines confirms the most abundant syncytin-1 expression in Mac-2A cell line. The densitometric values of syncytin-1 gp73 normalized against β-actin were 1 (Mac-1), 1.71 (Mac-2A), 1 (MyLa), and 0.98 (BeWo). The corresponding values for syncytin-1 gp63 were 0.61, 1.83, 0.56, and 0, respectively. The right-hand panel shows syncytin-1 expression silencing in BeWo cells using Dox to induce shSyn. BeWo, chorion carcinoma; CTCL, cutaneous T-cell lymphoma; Dox, doxycycline; Mac-1, lymphomatoid papulosis; Mac-2A, primary cutaneous anaplastic large cell lymphoma; MyLa, mycosis fungoides; pTIP, control plasmid; shSyn, short hairpin RNA knockdown.

papulosis (Mac-1), primary cutaneous anaplastic large cell lymphoma (Mac-2A), and also in the BeWo cell line, which is known to express syncytin-1 (Cheynet et al., 2005). Normal T cells showed only very limited syncytin-1 expression (Figure 1a) (Sun et al., 2016). To analyze the presence of syncytin-1 as cargo of EVs, we isolated EVs from the cell culture medium of the aforementioned cell lines using ultracentrifugation. Upon isolation, nanoparticle tracking analysis was employed to determine the amount and size distribution of cell-derived EVs (Supplementary Figure S2). The content of the EVs was subsequently analyzed by western blotting with syncytin-1-specific antibody and antibodies against HSP70, RAB5, and TSG101 to confirm the specificity of EVs (Figure 2a). Syncytin-1 protein was detected on the surface of EVs as confirmed by immunoelectron microscopy (Figure 2b).

The full-length transmembrane 73 kDa syncytin-1 protein (composed of surface and transmembrane subunits) was most prominent in the three CTCL cell lines and in the reference BeWo cell line, whereas an additional 63 kDa form was detected in the CTCL cell lines only (Figure 1b). This 63 kDa variant could represent a partially glycosylated protein or a cell type-specific splicing variant, since the expression of endogenous retroviral glycoproteins is known to be controlled by tissue-specific pre-mRNA splicing (Trejbalová et al., 2011). Moreover, EVs derived from the CTCL and BeWo cell lines

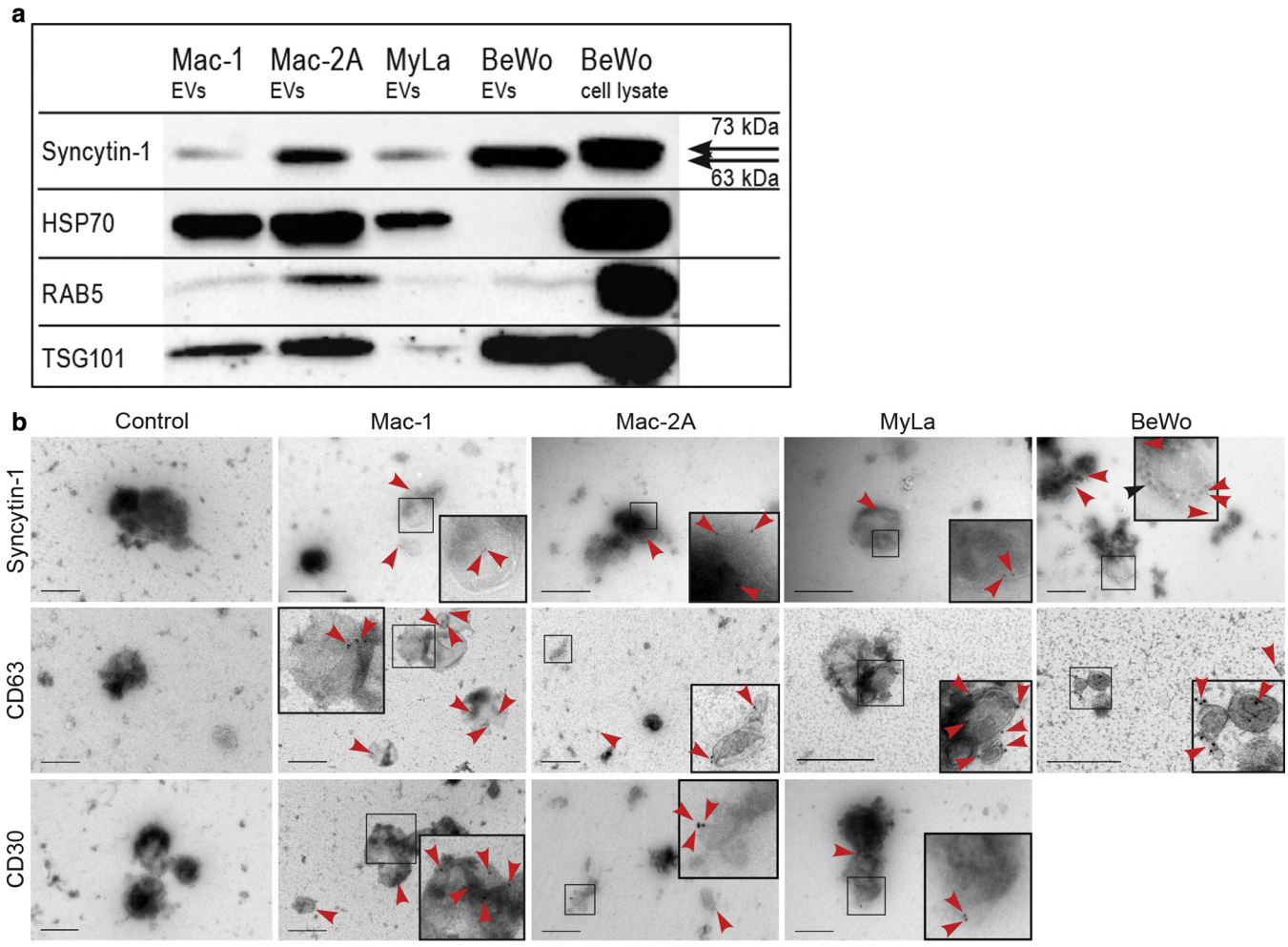

Figure 2. Syncytin-1 is detected on EVs derived from CTCL cell lines and BeWo cells. (**a**) EV-derived syncytin-1 is most prominently detected in the Mac-2A and BeWo cell lines by western blot analysis. The molecular weight of EV-derived syncytin-1 is 63 kDa, while the BeWo cell line lysate includes the full-length gp73 form. HSP70, RAB5, and TSG101 identify EVs. (**b**) Immunoelectron microscopy confirms syncytin-1 on EVs by 5 nm colloidal gold particles. The 15 nm gold particles (red arrowheads) depict the CD63 marker of EVs. The BeWo-derived EVs are typified as 50 nm vesicles with a phospholipid layer and electron-dense inner layer (black arrow). The bottom panel shows CD30 in CTCL cell line-derived EVs (15 nm gold particles, red arrowheads). The negative controls are immunostained without primary antibodies. Bar = 500 nm. BeWo, chorion carcinoma; CTCL, cutaneous T-cell lymphoma; EV, extracellular vesicle; Mac-1, lymphomatoid papulosis; Mac-2A, primary cutaneous anaplastic large cell lymphoma; MyLa, mycosis fungoides.

harbored only the 63 kDa syncytin-1 form. Several studies have reported changes in the glycosylation patterns of EVs in pathological conditions (Yáñez-Mó et al., 2015). Further studies are needed to investigate if this size variation of syncytin-1 plays a specific role in the pathomechanism of CTCL. In addition, we observed the most abundant syncytin-1 expression in Mac-2As and their EVs. This possibly reflects an advanced disease stage, since Mac-2A was established from the same patient as Mac-1 after progression to an aggressive primary cutaneous anaplastic large cell lymphoma. A knockdown study of syncytin-1 in the BeWo cell line verified the specificity of syncytin-1 antibody used for immunoblotting (Figure 1b, right panel).

In preliminary assays to assess the fusogenic effect of syncytin-1 on T cells, we transiently transfected HEK293T cells with phCMV plasmids encoding either human nonfusogenic (gp60) or fusogenic (env) syncytin-1 proteins. We hypothesized that upon expression in cells, these proteins would be captured in EVs released from the cells. Supernatants collected and cleared of transfected HEK293T cells were then applied onto the Jurkat T-cell leukemia cells, and the cell size was analyzed by flow cytometry 24 hours later. We observed an almost two-fold increase in the amount of large cells upon treatment with the supernatant harvested from fusogenic env-transfected cells compared with the nonfusogenic gp60 (Supplementary Figure S3a). Jurkat cells grown 48 hours in the supernatant from env-transfected cells formed plasma membrane-enveloped giant cells, which were undetectable in the control gp60-treated cells (Supplementary Figure S3b).

In addition to syncytin-1, we also studied the eventual release of the tumor-associated antigen CD30 (Figure 1a) in EVs. CD30 has been detected in EVs released by Hodgkin's lymphoma cells. CD30 communicates with bystander cells to allow the indirect binding of brentuximab vedotin, a monoclonal anti–CD30 antibody-drug

conjugate also effective in the treatment of MF (Hansen et al., 2016; Whittaker et al., 2016). Using immunoelectron microscopy, we detected and confirmed CD30 expression in the CTCL cell line-released EVs (Figure 2b). Thus, our observations are analogous to those in Hodgkin's lymphoma and may be relevant for the favorable clinical responses even in immunohistologically CD30-negative MF cases (Welborn and Duvic, 2019).

Taken together, the presence of syncytin-1, a fusogen, and its receptors in several CTCL cell lines, refers to its potential role in cancer cell fusion mechanisms, similar to the one used by placental trophoblasts (Bastida-Ruiz et al., 2016). We show that tumor cell-secreted EVs carry syncytin-1 protein, which may be transferred to recipient cells by the EVs to mediate membrane fusion and transfer tumor cell signals. Thus, we propose that studies on the content and biological function of EVs in CTCL patients will be of pivotal importance in developing novel therapeutic regimens for the currently incurable CTCL pathologies.

Data availability statement

The data analyzed during this study are included in this published article and its supplementary information files.

ORCIDs

Kirsi Laukkanen: https://orcid.org/0000-0001-6243-9850
Mirjam Saarinen: https://orcid.org/0000-0002-6345-3790
Francois Mallet: https://orcid.org/0000-0002-1331-096X
Maria Aatonen: https://orcid.org/0000-0002-4819-6722
Annika Hau: https://orcid.org/0000-0002-3388-3394
Annamari Ranki: https://orcid.org/0000-0003-4335-0396

CONFLICT OF INTEREST

FM is an employee of an in vitro diagnostic company. The remaining authors state no conflict of interest.

ACKNOWLEDGMENTS

We thank Mrs. Alli Tallqvist and Ms. Inga Liukko for their skillful technical assistance. We thank Professor Robert Gniadecki, Bispebjerg Hospital, Copenhagen University, for the kind gift of the MyLa, Mac-1, and Mac-2A cell lines. We thank the Extracellular Vesicle Core Facility at the University of Helsinki, Finland, for providing nanoparticle tracking analysis and preparation of immunoelectron microscopy samples. Biomedicum Imaging Unit and Biomedicum Flow Cytometry Core facilities at the University of Helsinki, Finland, were used for imaging and flow cytometry analyses. This work was supported by grants from the Cancer Foundation Finland and the Finnish Dermatological Society.

AUTHOR CONTRIBUTIONS

Conceptualization: AR, KL; Data curation: KL, AH; Formal analysis: KL, AH; Funding acquisition: AR; Investigation: KL, AH, MS, MA; Methodology: KL, AH, AR; Project Administration: AR; Resources: AR, FM; Supervision: AR, FM; Validation: KL, AH, MA; Visualization: KL, AH; Writing - Original Draft: AR, KL, AH; Writing - Review & Editing: KL, FM, AH, MS, MA, and AR.

Kirsi Laukkanen[1,*], Mirjam Saarinen[1], Francois Mallet[2,3], Maria Aatonen[4], Annika Hau[1] and Annamari Ranki[1]

[1]Department of Dermatology and Allergology, Clinicum, University of Helsinki and Helsinki University hospital, Helsinki, Finland; [2]Joint Research Unit, Hospice Civils de Lyon, bioMerieux, Centre Hospitalier Lyon Sud, Pierre-Benite, France; [3]EA 7426 Pathophysiology of Injury-induced Immunosuppression, University of Lyon1-Hospices Civils de Lyon-bioMérieux, Hôpital Edouard Herriot, Lyon, France; and [4]EV Core and Molecular and Integrative Biosciences Research Programme, Faculty of Biological and Environmental Sciences, University of Helsinki, Helsinki, Finland

[*]Corresponding author e-mail: kirsi.laukkanen@helsinki.fi

SUPPLEMENTARY MATERIAL

Supplementary material is linked to the online version of the paper at www.jidonline.org, and at https://doi.org/10.1016/j.jid.2019.11.021.

REFERENCES

Bastida-Ruiz D, Van Hoesen K, Cohen M. The dark side of cell fusion. Int J Mol Sci 2016;17:638.

Bjerregaard B, Holck S, Christensen IJ, Larsson LI. Syncytin is involved in breast cancer-endothelial cell fusions. Cell Mol Life Sci 2006;63:1906–11.

Cheynet V, Ruggieri A, Oriol G, Blond JL, Boson B, Vachot L, et al. Synthesis, assembly, and processing of the env ERVWE1/syncytin human endogenous retroviral envelope. J Virol 2005;79:5585–93.

Hansen HP, Trad A, Dams M, Zigrino P, Moss M, Tator M, et al. CD30 on extracellular vesicles from malignant Hodgkin cells supports damaging of CD30 ligand-expressing bystander cells with brentuximab-vedotin, in vitro. Oncotarget 2016;7:30523–35.

Maas SLN, Breakefield XO, Weaver AM. Extracellular vesicles: unique intercellular delivery vehicles. Trends Cell Biol 2017;27:172–88.

Maliniemi P, Vincendeau M, Mayer J, Frank O, Hahtola S, Karenko L, et al. Expression of human endogenous retrovirus-w including syncytin-1 in cutaneous T-cell lymphoma. PLOS ONE 2013;8:e76281.

Nikolaenko L, Zain J, Rosen ST, Querfeld C. CD30-positive lymphoproliferative disorders. Cancer Treat Res 2019;176:249–68.

Prada I, Meldolesi J. Binding and fusion of extracellular vesicles to the plasma membrane of their cell targets. Int J Mol Sci 2016;17:1296.

Strick R, Ackermann S, Langbein M, Swiatek J, Schubert SW, Hashemolhosseini S, et al. Proliferation and cell-cell fusion of endometrial carcinoma are induced by the human endogenous retroviral syncytin-1 and regulated by TGF-beta. J Mol Med (Berl) 2007;85:23–38.

Sun Y, Zhu H, Song J, Jiang Y, Ouyang H, Huang R, et al. Upregulation of leukocytic syncytin-1 in acute myeloid leukemia patients. Med Sci Monit 2016;22:2392–403.

Trejbalová K, Blazková J, Matousková M, Kucerová D, Pecnová L, Vernerová Z, et al. Epigenetic regulation of transcription and splicing of syncytins, fusogenic glycoproteins of retroviral origin. Nucleic Acids Res 2011;39:8728–39.

Welborn M, Duvic M. Antibody-based therapies for cutaneous T-cell lymphoma. Am J Clin Dermatol 2019;20:115–22.

Whittaker S, Hoppe R, Prince HM. How I treat mycosis fungoides and sezary syndrome. Blood 2016;127:3142–53.

Willemze R, Cerroni L, Kempf W, Berti E, Facchetti F, Swerdlow SH, et al. The 2018 update of the WHO-EORTC classification for primary cutaneous lymphomas. Blood 2019;133:1703–14.

Yáñez-Mó M, Siljander PR, Andreu Z, Zavec AB, Borràs FE, Buzas EI, et al. Biological properties of extracellular vesicles and their physiological functions. J Extracell Vesicles 2015;4:27066.

SUPPLEMENTARY MATERIAL AND METHODS

Cell lines

We used CTCL cell lines representing MF (MyLa cell line), lymphomatoid papulosis (Mac-1), and primary cutaneous anaplastic large cell lymphoma (Mac-2A) (Netchiporouk et al., 2017). The Mac-1 cell line is derived from circulating Sézary-like cells in the peripheral blood of a patient with indolent lymphomatoid papulosis, while Mac-2A was established from skin tumor nodules of the same patient after progression to aggressive primary cutaneous anaplastic large cell lymphoma (Davis et al., 1992). Although clonally related, Mac-1 and Mac-2A are genomically and transcriptionally distinct (Ehrentraut et al., 2013).

The MF-derived cell line MyLa and human embryonic kidney cell line HEK293T were grown in DMEM supplemented with Glutamax, penicillin-streptomycin, and 10% fetal bovine serum (FBS) (Gibco, Thermo Fisher Scientific, Waltham, MA). The Mac-1 and Mac-2A cell lines were grown in RPMI 1640 medium supplemented with Glutamax, penicillin-streptomycin, and 10% FBS. The human BeWo chorioncarcinoma cell line was maintained in Ham's F12 medium supplemented with Glutamax, penicillin-streptomycin, and 10% FBS. Normal T cells were isolated from a buffy coat of a healthy blood donor (Finnish Red Cross Blood Service, Helsinki, Finland) with the Lympholyte-H gradient separation method (CL5015, Cedarlane Corporation, Burlington, ON, Canada) followed by enrichment with a Pan T cell Isolation Kit (130-096-535, Milteney Biotec, Auburn, CA) according to the manufacturer's instructions. The enriched cells were immunostained with CD3 and CD19 antibodies and analyzed by flow cytometry (Biomedicum Flow Cytometry Core, Helsinki, Finland) and immunocytochemistry staining with CD3 antibody (MF7254, Dako, Glostrup, Denmark) to confirm the T cell nature of the enriched cells (data not shown). The cell lines were authenticated at the Finnish Institute for Molecular Medicine, Helsinki, Finland, and tested routinely for mycobacterial contamination using a MycoAlert Mycoplasma Detection Kit (LT07, Lonza, Basel, Switzerland).

Immunocytochemistry

Immunocytochemistry was used to the detect expression of syncytin-1 (1:25, SC-50369, Santa Cruz Biotechnology, Santa Cruz, CA), ASCT-1 (1:25 or 1:5, SC-134846, Santa Cruz Biotechnology), and ASCT-2 (1:25, 5100, Cell Signaling Technology, Leiden, Netherlands) in cytocentrifuge preparations of Mac-1, Mac-2A, Myla, BeWo, and T cells. Anti−CD30 antibody (1:400, 134080, Abcam, Cambridge, UK) was used to detect CD30 expression on CTCL and BeWo cells. The ImmPRESS Reagent kit (MP-7500, Vector Laboratories, Burlingame, CA) was used according to the manufacturer's instructions. NovaRed (SK-4800, Vector Laboratories) and Mayer's hemalum solution (Merck, Darmstadt, Germany) were used as chromogens for ASCT-1/ASCT-2 receptors and CD30. Horseradish Peroxidase Green substrate buffer (KDB-10049, Nordic BioSite, Täby, Sweden) and Nuclear Fast red (60700 Sigma-Aldrich, Darmstadt, Germany) were used for syncytin-1.

EV purification and analyses

Ultracentrifugation was used to isolate the EVs. Cell lines were grown for 72 hours in supplemented media as described above, but 10% EV-depleted FBS was used. FBS was depleted from EV using polyethylene glycol (PEG). Heat-inactivated FBS (Gibco, Thermo Fisher Scientific) was treated with PEG (P6667, Sigma-Aldrich, St. Louis, MO). A sterile-filtered (0.2 μm filter) 50% (w/v) stock solution of PEG prepared in 1× Dulbecco's phosphate buffered saline (PBS) was protected from light and stored at 4 °C. The FBS and PEG stock solutions were mixed in a 5:1 ratio by gently inverting 5 to 10 times and incubated for 2 hours at 4 °C protected from light before centrifugation for 30 minutes at 4 °C at 1,500*g* in a swinging-bucket rotor. The supernatant was collected leaving a layer of at least 0.5 cm on top of the pellet, and sterile filtered (0.1 μm filter) into aliquots stored at −20 °C until use. For EV purification, cell supernatants were centrifuged at 3,000*g* at 4 °C for 25 minutes, followed by centrifugation at 100,000*g* at 4 °C for 2 hours to isolate the microvesicle and exosome fractions. EV pellets were washed with 0.1 μm filtered Dulbecco's PBS, followed by centrifugation at 100,000*g* at 4 °C for 2 hours. Purified EV samples were analyzed by nanoparticle tracking analysis using Nanosight model LM14 (Malvern Panalytical Ltd, Malvern, United Kingdom) equipped with blue (404 nm, 70 mW) laser and a Scientific Complementary metal-oxide-semiconductor camera. The samples were diluted in Dulbecco's PBS, and three 60-second videos were recorded using camera level 13. The data were analyzed using Nanoparticle Tracking Analysis software 3.0 (Malvern Panalytical Ltd).

Western blot analyses of cell lines and EVs

Mac-1, Mac-2A, MyLa, and BeWo cells were harvested either by centrifugation or mechanical scraping and washed twice with ice-cold PBS. Cell pellets were resuspended in 1× PBS buffer/0.5% Triton X-100 with EDTA-free protease inhibitors (Roche, Basel, Switzerland) and incubated on ice for 60 minutes. The protein concentration was determined using the DC protein assay kit (Bio-Rad, Göteborg, Sweden). A total of 30 μg and 40 μg of protein was used for ASCT-1/ASCT-2 and syncytin-1 western blot analyses, respectively. The samples were boiled at 95 °C for 5 minutes in Laemmli Sample Buffer (Bio-Rad) with 2-mercaptoethanol. Protein lysates were separated by 10% SDS-PAGE electrophoresis and transferred onto a nitrocellulose membrane (Whatman, Boston, MA) at 100 V for 90 minutes. Membranes were incubated with anti−ASCT-1 (1:200, SC-134846, Santa Cruz Biotechnology), anti−ASCT-2 (1:200, 5100, Cell Signaling Technology), and anti−syncytin-1 (1:200, SC-50369, Santa Cruz Biotechnology) antibodies overnight at 4 °C. Incubation with anti−β-actin antibodies (4970L, 1:1,000, Cell Signaling Technology) served as a loading control. After washing, the membranes were incubated with anti−rabbit horseradish peroxidase-conjugated secondary antibody (PO448, Dako) for 1 hour at room temperature. The proteins were detected using Clarity ECL reagent (Bio-Rad), and expression values were normalized

against β-actin using the ChemiDoc MP Imaging System (Bio-Rad). Adjusted density values were calculated using Image Lab software (Bio-Rad). Western blot analyses of EVs were performed using 5 μg of protein. The samples were boiled at 95 °C for 5 minutes in Laemmli Sample Buffer (Bio-Rad) with 2-mercaptoethanol and additional SDS (total 8%). Protein lysates were separated as described above. In addition to probing with anti−syncytin-1 antibody, anti−HSP70 (1:500, 610608, BD Biosciences, San Jose, CA), anti−RAB5 (1:100, PA5-29022, ThermoFisher Scientific), and anti−TSG101 (1:100, MA1-23296, ThermoFisher Scientific) antibodies were used as EV-specific markers, followed by incubation with anti−rabbit or anti−mouse horseradish peroxidase-conjugated secondary antibody (PO448 or PO447, Dako).

Knockdown assay of syncytin-1

BeWo cells were transduced with pTIP and pTIP-short hairpin RNA knockdown lentiviruses and selected using 3 μg/ml puromycin (Sigma-Aldrich, St. Louis, MO) to stably express either control plasmid (pTIP) or a TetON-inducible short hairpin RNA knockdown construct against syncytin-1 (pTIP-short hairpin RNA knockdown). The vectors were kindly provided by Dr Marcus Peter, Northwestern University, Chicago, IL, and published by Hau et. al. (2012). The sequence of the knockdown oligo was already published by Aagaard et al. (2012). The expression of Syncytin-1 short hairpin RNA was induced using 100 ng/ml doxycycline (Sigma-Aldrich, St. Louis, MO) for 10 days. Cells were then lysed and probed for syncytin-1 using Santa Cruz anti−syncytin-1 antibody (SC-50369, Santa Cruz Biotechnology).

Immunoelectron microscopy

EV samples from cell lines were prepared for electron microscopy and imaged as previously described (Puhka et al., 2017) with the addition of an immunostaining step. Briefly, after being loaded onto 200 mesh copper grids, the samples were permeabilized with 0.01% saponin with a prefixation of 2% paraformaldehyde. The samples were then incubated with or without (negative control) anti−syncytin-1 antibody (1:100, SC-50369, Santa Cruz Biotechnology) and anti−CD30 antibody (1:400, 134080, Abcam) followed by 5 nm or 15 nm colloidal gold conjugated goat-anti−rabbit-IgG (1:150, BBI Solutions, Cardiff, UK), respectively. Next, a post-fixation step with 1% glutaraldehyde was performed. In addition, anti−CD63 staining was performed as an EV-specific control. The samples were blocked and incubated with anti−CD63 antibody (1:250, Pelicluster, Sanquin, Amsterdam, The Netherlands) followed by 10-nm colloidal gold conjugated goat-anti−mouse-IgG secondary antibody (1:80, BBI Solutions). All the samples were viewed with transmission electron microscopy using Jeol JEM-1400 (Jeol Ltd, Tokyo, Japan). Images were taken with a Gatan Orius SC 1000B CCD-camera (Gatan Inc, Pleasanton, CA).

Cell fusion assay of syncytin-1

Human embryonic kidney HEK293T cells were seeded a day before transfection. On the day of transfection, DMEM-containing EV-depleted FBS (centrifuged at 100,000*g* for 18 hours) was placed onto cells, and the cells were transfected with 1.5 μg of plasmids according to manufacturer's instructions using Lipofectamine 2000 (Thermo LifeSciences, Carlsbad, CA). The nonfusogenic recombinant form of pcDNA−CMV-human gp60 syncytin-1 (hydrophobic tail deleted and RNKR cleavage site mutated) (Antony et al., 2007) and fusogenic pcDNA−CMV-human env syncytin-1 plasmids were used (a kind gift from Dr. Francois Mallet, BioMerieux, France). Approximately 6 hours after the addition of lipofectamine complexes, media were replaced and supplemented with EV-depleted FBS. The following day, media from each transfection were harvested, and cells and debris were removed by centrifugation (860*g* for 5 minutes). Jurkat cells were counted, and 80,000 to 200,000 cells were resuspended into media harvested from the transfected HEK293T cells. Approximately 24 hours later, the Jurkat cells were harvested, fixed for 30 minutes at room temperature with 2% paraformaldehyde in PBS, and rinsed and stored at 4 °C until FACS analysis. In a parallel experiment, Jurkat cells were incubated with supernatants for 48 hours, and photomicrographs were taken. Cell-size analysis was performed using a BD Accuri C6 (BD Biosciences, San Jose, CA) and FlowJo version 10.5.3. (Treestar Inc, Ashland, OR). The cell size was determined by setting a gate to exclude the normal-sized cells of the control sample and only quantifying the cells that were in this "large" gate, specifically cells that had increased forward scatter or side scatter (Hadji et al., 2014).

SUPPLEMENTARY REFERENCES

Aagaard L, Bjerregaard B, Kjeldbjerg AL, Pedersen FS, Larsson LI, Rossi JJ. Silencing of endogenous envelope genes in human choriocarcinoma cells shows that envPb1 is involved in heterotypic cell fusions. J Gen Virol 2012;93:1696−9.

Antony JM, Ellestad KK, Hammond R, Imaizumi K, Mallet F, Warren KG, et al. The human endogenous retrovirus envelope glycoprotein, syncytin-1, regulates neuroinflammation and its receptor expression in multiple sclerosis: A role for endoplasmic reticulum chaperones in astrocytes. J Immunol 2007;179:1210−24.

Davis TH, Morton CC, Miller-Cassman R, Balk SP, Kadin ME. Hodgkin's disease, lymphomatoid papulosis, and cutaneous T-cell lymphoma derived from a common T-cell clone. N Engl J Med 1992;326:1115−22.

Ehrentraut S, Nagel S, Scherr ME, Schneider B, Quentmeier H, Geffers R, et al. t(8;9)(p22;p24)/PCM1-JAK2 activates SOCS2 and SOCS3 via STAT5. PLOS ONE 2013;8:e53767.

Hadji A, Ceppi P, Murmann AE, Brockway S, Pattanayak A, Bhinder B, et al. Death induced by CD95 or CD95 ligand elimination. Cell Rep 2014;7:208−22.

Hau A, Ceppi P, Peter ME. CD95 is part of a let-7/p53/miR-34 regulatory network. PLOS ONE 2012;7:e49636.

Netchiporouk E, Gantchev J, Tsang M, Thibault P, Watters AK, Hughes JM, et al. Analysis of CTCL cell lines reveals important differences between mycosis fungoides/sezary syndrome vs. HTLV-1^+ leukemic cell lines. Oncotarget 2017;8:95981−98.

Puhka M, Nordberg ME, Valkonen S, Rannikko A, Kallioniemi O, Siljander P, et al. KeepEX, a simple dilution protocol for improving extracellular vesicle yields from urine. Eur J Pharm Sci 2017;98:30−9.

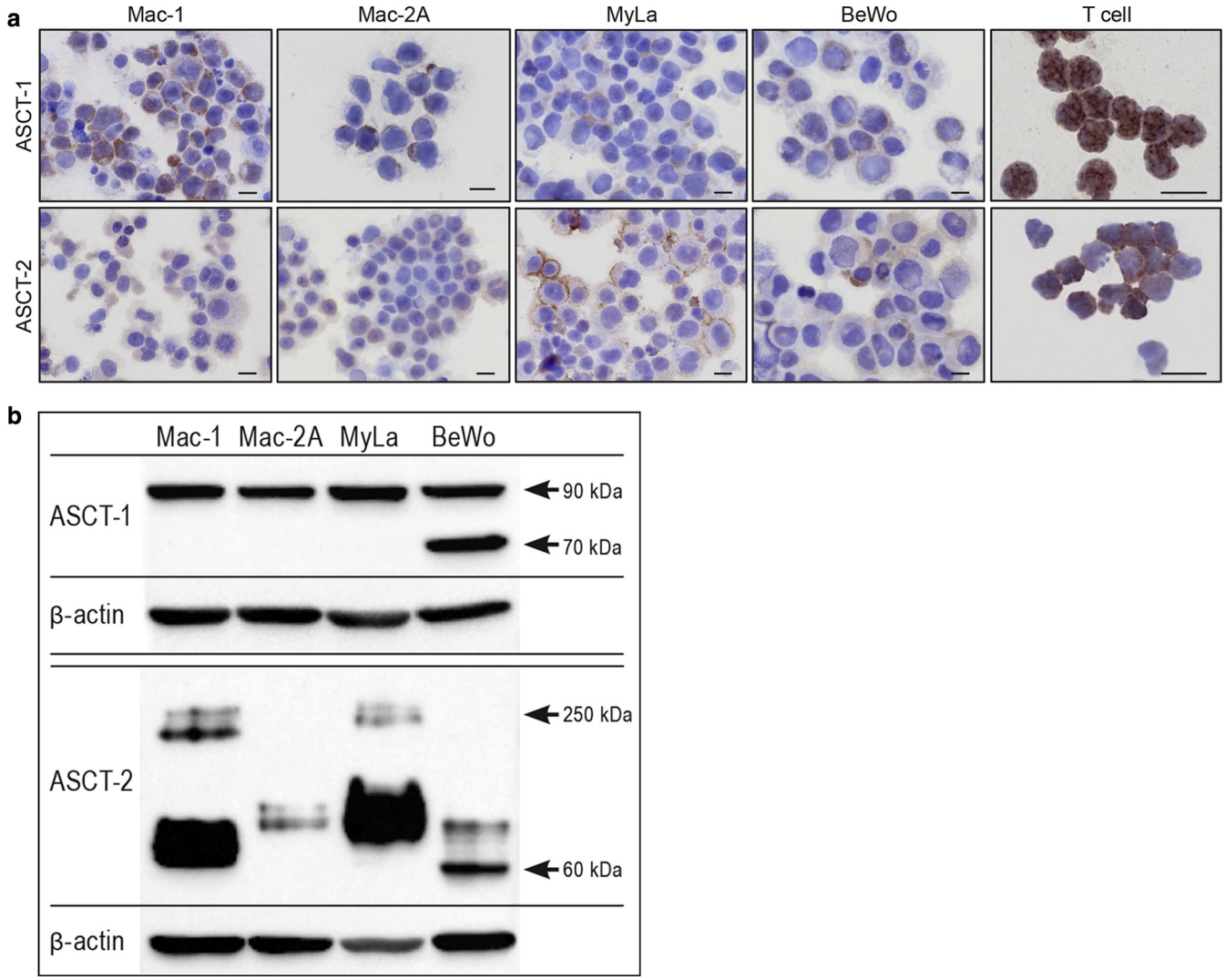

Supplementary Figure S1. Syncytin-1 receptors ASCT-1 and ASCT-2 (sodium-dependent neutral amino acid transporter types 1 and 2) are expressed in CTCL, BeWo chorion carcinoma, and T cells. (**a**) Expression of ASCT-1 and ASCT-2 in Mac-1 (lymphomatoid papulosis), Mac-2A (primary cutaneous anaplastic large cell lymphoma), MyLa (mycosis fungoides), BeWo (chorion carcinoma) cell lines and in normal, enriched T cells as detected by immunocytochemistry with anti—ASCT-1 and anti—ASCT-2 antibodies (dark brown). Bar = 20 μm. (**b**) Western blot analysis of ASCT-1 and ASCT-2 expressed by the CTCL and BeWo cell lines described above. The 90 kDa and 70 kDa bands in the upper panel represent ASCT-1 proteins of differing glycosylation; the molecular weight of ASCT-1 is 56 kDa. In the lower panel, ASCT-2 molecular weights vary between 60 kDa and 250 kDa and represent forms with differing glycosylation. CTCL, cutaneous T-cell lymphoma.

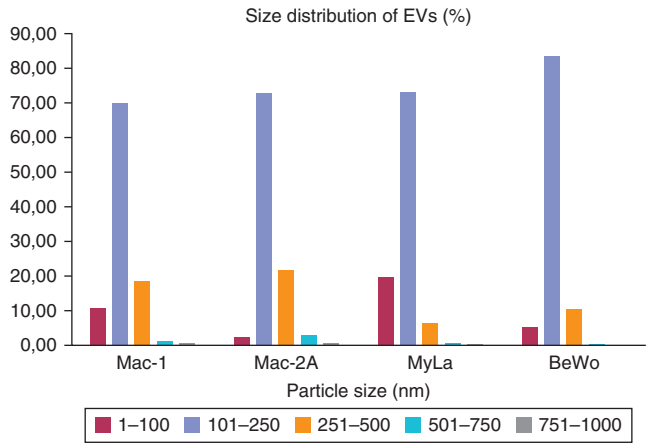

Supplementary Figure S2. Size distribution of EVs (%). Nanoparticle tracking analysis of CTLC and BeWo cell line-derived EVs shows a size range of 101 to 250 nm to be the most abundant. The large 751 to 1,000 nm vesicles are absent from BeWo cell line-derived EVs. CTCL, cutaneous T-cell lymphoma; Ev, extracellular vesicle.

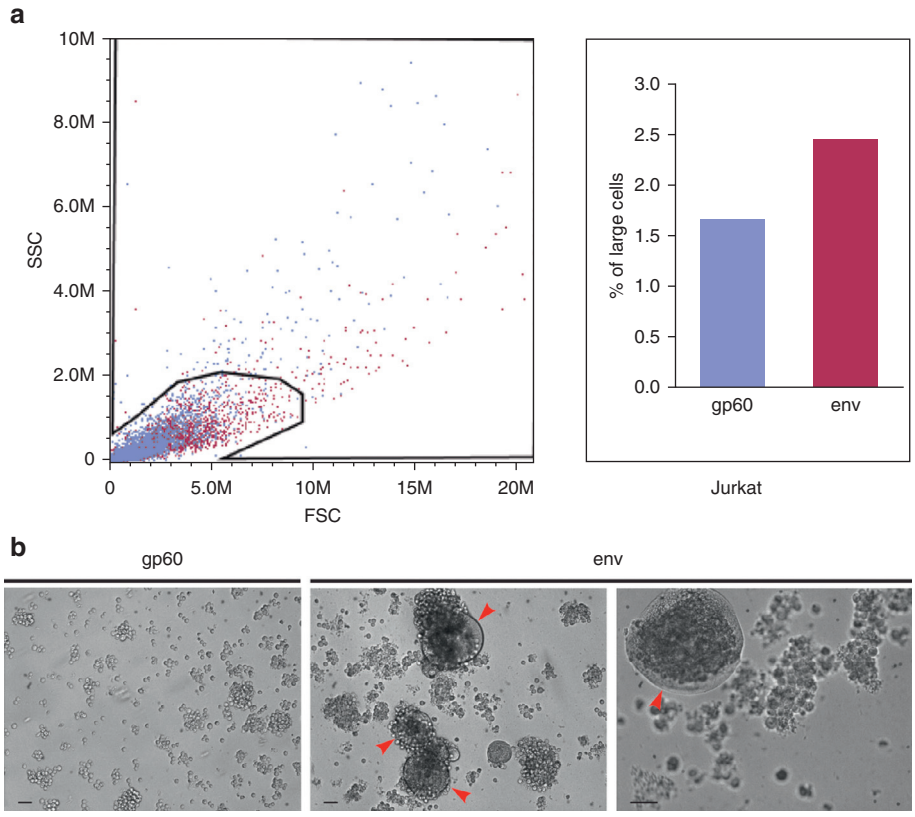

Supplementary Figure S3. Transfected and secreted fusogenic syncytin-1 increases cell size and induces fusions. (**a**) Size distribution of Jurkat T-cell leukemia cells treated with media from HEK293T cells transfected with either gp60 (blue trace) or env (red trace). Media from env-transfected HEK293T cells mediate the cell size increase of Jurkat cells as determined by flow cytometry. FSC represents granulocity, and SSC represents cell size. (**b**) Photomicrographs of Jurkat cells treated with media containing gp60 (left) and env (middle and right). Red arrows indicate plasma membrane-enveloped giant fusion cells. Bar = 40 μm. env, fusogenic particles; FSC, forward scatter; gp60, nonfusogenic particles; SSC, side scatter.